Drug Design, Development and Therapy

Dovepress
open access to scientific and medical research

Open Access Full Text Article

ORIGINAL RESEARCH

Formononetin, an active compound of *Astragalus membranaceus* (Fisch) Bunge, inhibits hypoxia-induced retinal neovascularization via the HIF-1α/VEGF signaling pathway

This article was published in the following Dove Press journal:
Drug Design, Development and Therapy
23 September 2016
Number of times this article has been viewed

Jianming Wu[1–3,*]
Xiao Ke[2,*]
Na Ma[2]
Wei Wang[2]
Wei Fu[2]
Hongcheng Zhang[2]
Manxi Zhao[2]
Xiaoping Gao[2]
Xiaofeng Hao[2]
Zhirong Zhang[3]

[1]Laboratory of Chinese Materia Medica, Department of Pharmacology, School of Pharmacy, Southwest Medical University, Luzhou, [2]Post-Doctoral Research Station, Kanghong Pharmaceutical Group, [3]Post-Doctoral Mobile Station, West China School of Pharmacy, Sichuan University, Chengdu, Sichuan, People's Republic of China

*These authors contributed equally to this work

Correspondence: Xiaofeng Hao
Post-Doctoral Research Station, Kanghong Pharmaceutical Group, No 36, Shuxi Road, Chengdu, Sichuan 610036, People's Republic of China
Tel +86 28 8751 9670
Email hxf@cnkh.com

Zhirong Zhang
Post-Doctoral Mobile Station, West China School of Pharmacy, Sichuan University, No 17, Section 3, South Renmin Road, Chengdu, Sichuan 610041, People's Republic of China
Tel +86 28 8550 1566
Email zrzzl@vip.sina.com

Background: It has been reported that formononetin (FMN), one of the main ingredients from famous traditional Chinese medicine "Huang-qi" (*Astragalus membranaceus* [Fisch] Bunge) for Qi-tonifying, exhibits the effects of immunomodulation and tumor growth inhibition via antiangiogenesis. Furthermore, *A. membranaceus* may alleviate the retinal neovascularization (NV) of diabetic retinopathy. However, the information of FMN on retinal NV is limited so far. In the present study, we investigated the effects of FMN on the hypoxia-induced retinal NV and the possible related mechanisms.

Materials and methods: The VEGF secretion model of acute retinal pigment epithelial-19 (ARPE-19) cells under chemical hypoxia was established by the exposure of cells to 150 μM $CoCl_2$ and then cells were treated with 3-(5′-hydroxymethyl-2′-furyl)-1-benzylindazole (YC-1, a potent HIF-1α inhibitor, 1.0 μg/mL) or different concentrations of FMN (0.2 μg/mL, 1.0 μg/mL, and 5.0 μg/mL). The supernatants of cells were collected 48 hours later to measure the VEGF concentrations, following the manufacturer's instruction. The mRNA expressions of VEGF, HIF-1α, PHD-2, and β-actin were analyzed by quantitative reverse transcription polymerase chain reaction, and the protein expressions of HIF-1α and PHD-2 were determined by Western blot analysis. Furthermore, the rats with retinopathy were treated by intraperitoneal administration of conbercept injection (1.0 mg/kg) or FMN (5.0 mg/kg and 10.0 mg/kg) in an 80% oxygen atmosphere. The retinal avascular areas were assessed through visualization of the retinal vasculature by adenosine diphosphatase staining and hematoxylin and eosin staining.

Results: FMN can indeed inhibit the VEGF secretion of ARPE-19 cells under hypoxia, downregulate the mRNA expression of VEGFA and PHD-2, and decrease the protein expression of VEGF, HIF-1α, and PHD-2 in vitro. Furthermore, FMN can prevent hypoxia-induced retinal NV in vivo.

Conclusion: FMN can ameliorate retinal NV via the HIF-1α/VEGF signaling pathway, and it may become a potential drug for the prevention and treatment of diabetic retinopathy.

Keywords: formononetin, angiogenesis, oxygen-induced retinopathy, vascular endothelial growth factor, hypoxia-inducible factor-1

Introduction

Astragalus membranaceus (Fisch) Bunge, known as Huang-qi in Chinese or Radix Astragali in Latin, is one of the most popular herbal medicines worldwide, and it has been widely used as a Qi-tonifying medicine in the People's Republic of China, Mongolia, and Korea for a long time.[1,2] Pharmacological studies have shown that

submit your manuscript | www.dovepress.com
Dovepress
http://dx.doi.org/10.2147/DDDT.S114022

A. membranaceus exhibits many beneficial effects, including immunomodulation,[3–5] antihyperglycemic effects and improved insulin sensitivity,[6–8] anti-inflammation effects,[9,10] antioxidant effects,[11,12] antiviral effects,[13,14] hepatoprotection effects,[15,16] antineoplastic effects, protection of cardiovascular function,[17] and so on. Meanwhile, phytochemical studies have displayed >100 compounds from *A. membranaceus* (root), such as flavonoids, polysaccharides, saponins, sucroses, amino acids, and phenolic acids.[1] Among them, formononetin (FMN; 7-hydroxy-4′-methoxyisoflavone), a flavonoid with neuroprotection,[18] anti-inflammation,[19] antiviral,[20] antiangiogenesis and tumor growth inhibition,[21] cardioprotection,[22] and other pharmacological effects, has been frequently used as the quality control marker of *A. membranaceus* and its preparations. Recently, it has been reported that some preparations mainly composed of *A. membranaceus*, such as Huangqi injection and Keluoxin capsule, could alleviate the retinal neovascularization (NV) of diabetic retinopathy (DR).[23,24] A previous study has clearly demonstrated that FMN from *A. membranaceus* has an inhibitory effect on the tumor growth via antiangiogenesis,[21] but it is still unknown whether FMN can inhibit hypoxia-induced retinal NV in the pathophysiologic process of DR.

DR is a common microvascular complication of patients with diabetes mellitus.[25] Retinal NV can induce vitreous hemorrhage and tractional retinal detachment, resulting in visual deterioration.[26] Furthermore, increased vascular permeability leads to macular edema in patients with DR.[27] Therefore, DR becomes the leading cause of blindness in the adults. Importantly, VEGF plays a critical role in the retinal NV of DR, which stimulates the proliferation and migration of vascular endothelial cells and increases vascular permeability.[28] Hypoxia is one of the most potent triggers of VEGF expression, acting on the processes of DNA transcription, mRNA stabilization, and translation and release of VEGF,[29] which is centrally controlled by the HIF-1α, a transcription factor that regulates hypoxia-inducible genes, including VEGFA, and induces an angiogenic response.[30] Therefore, HIF-1α is increased to induce the expression of VEGF under hypoxia, resulting in increased vascular permeability and retinal NV. On the other hand, inhibition of HIF-1α can prevent the retinal NV in the condition of hypoxia.[31–33] These studies indicate that HIF-1α/VEGF signaling pathway plays the key role in the retinal NV of DR. In the present study, we investigated the preventive effect of FMN on retinal NV from secretion of VEGF in the acute retinal pigment epithelial-19 (ARPE-19) cells induced by $CoCl_2$ in vitro and NV of oxygen-induced retinopathy of a rat model in vivo.

Materials and methods

Reagents and antibodies

Conbercept injection (Lot: 20110610B) was provided by Chengdu Kanghong Pharmaceutical Group Co., Ltd. (Chengdu, Sichuan, People's Republic of China). FMN (Lot: 20100311) was purchased from Jubang Biotechnology Co., Ltd. (Chengdu, Sichuan, People's Republic of China) and dissolved in dimethyl sulfoxide (DMSO) to make a stock solution of 10.0 mg/mL. Human VEGF enzyme-linked immunosorbent assay (ELISA) kits (Lot: DVE00) were provided by R&D Systems Inc. (Minneapolis, MN, USA). Dulbecco's Modified Eagle's Medium (DMEM)/F12 medium, fetal bovine serum (FBS), and trypsin–ethylenediaminetetraacetic acid (EDTA) solution were purchased from Thermo Fisher Scientific (Waltham, MA, USA). Tetramethylethylenediamine, DMSO, adenosine diphosphate (ADP), and ammonium sulfide were purchased from Sigma-Aldrich Co. (St Louis, MO, USA). The 5-[1-(phenylmethyl)-1H-indazol-3-yl]-2-furanmethanol (YC-1), anti-HIF-1α antibody, and anti-PHD-2 antibody were obtained from Abcam (Cambridge, MA, USA). PrimeScript RT reagent kit with gDNA Eraser and SYBR Premix Ex Taq™ were purchased from Takara-Bio (Kusatsu, Shiga, Japan).

Cell culture

A human ARPE-19 cell line (Lot: 60279299) was purchased from the American Type Culture Collection (Manassas, VA, USA), and the cells were cultured in DMEM/F12 medium with 10% FBS, 100 units/mL penicillin, and 100 μg/mL streptomycin in an incubator at 37°C with 5% CO_2. After 90% confluence, the cells were digested by 0.25% trypsin–0.02% EDTA for passage.

Determination of VEGF secretion by ARPE-19 cells under chemical hypoxia

According to the previous report from the literature,[28] ARPE-19 cells were seeded into 96-well plates at a density of 8×10^3 cells/well. After being cultured for 24 hours, the culture medium was replaced with fresh FBS-free DMEM/F12 medium. Then, the cells were treated with 1.0 μg/mL YC-1 and different concentrations of FMN (0.2 μg/mL, 1.0 μg/mL, and 5.0 μg/mL). The cells in the control group were treated with the culture medium containing the same concentration of DMSO as in the FMN solution. A total of 150 μM of $CoCl_2$ was added to mimic hypoxic condition after 24 hours. The cells treated with DMSO-containing medium were used as control, and those treated with $CoCl_2$ and YC-1 as positive controls. Conditioned medium was collected 48 hours later

and centrifuged at 800× *g* for 5 minutes, and the supernatants were transferred to vials and stored at −80°C for further analysis. All experiments were performed in triplicate.

The concentrations of VEGF protein in the conditioned media were measured using the human VEGF Quantikine ELISA kits according to the manufacturer's instruction. Absorbance values (450 nm) were recorded in triplicate with a microplate reader (SpectraMax M_5; Molecular Devices LLC, Sunnyvale, CA, USA). The concentrations of VEGF were calculated from the standard curve. The sensitivity of the VEGF kits was 5.0 pg/mL.

RNA isolation and analysis of the mRNA expressions of VEGF, HIF-1α, and PHD-2

ARPE-19 cells were plated at a density of 1×10^5 cells/well in six-well plates, allowed to adhere overnight, and then treated with YC-1 (1.0 μg/mL) or different concentrations of FMN (0.2 μg/mL, 1.0 μg/mL, and 5.0 μg/mL). After being cultured for 24 hours, the culture media were withdrawn, and the cells were washed with cold phosphate-buffered saline before harvest. The cell pellets were collected for mRNA extraction after microcentrifuging at 800× *g* for 5 minutes at 4°C. Total RNA from the ARPE-19 cells was isolated with the TRIzol reagent. cDNA was synthesized with a cDNA synthesis kit according to the manufacturer's protocol. The relative levels of each gene mRNA transcripts to β-actin were determined by quantitative reverse transcription polymerase chain reaction (qRT-PCR) using the SYBR premixed system and specific primers. The primer sequences for VEGFA, HIF-1α, PHD-2, and β-actin were as follows: homo VEGFA 5′-CGA AAC CAT GAA CTT TCT GC-3′ (forward) and 5′-CCT CAG TGG GCA CAC ACT CC-3′ (reverse), homo HIF-1α 5′-ACA AGT CAC CAC AGG ACA G-3′ (forward) and 5′-AGG GAG AAA ATC AAG TCG-3′ (reverse), homo PHD-2 5′-AAA CCA TTG GGC TGC TCA T-3′ (forward) and 5′-CGT ACA TAA CCC GTT CCA TTG-3′ (reverse), and homo β-actin 5′-AGC GGG AAA TCG TGC GTG AC-3′ (forward) and 5′-AGT TTC GTG GAT GCC ACA GGA C-3′ (reverse). qRT-PCR was performed by Opticon 3 continuous fluorescence detector (MJ Research, Inc., Waltham, MA, USA). The comparative cycle of threshold fluorescence (C_t) method was used, and the relative transcript amount of the target gene was normalized to that of β-actin using the $2^{-\Delta\Delta C_t}$ method.

Western blot analysis of the proteins of HIF-1α and PHD-2

ARPE-19 cells were seeded at a density of 2.0×10^5 cells/bottle in culture bottles, and the cells were treated with YC-1 (1.0 μg/mL) or different concentrations of FMN (0.2 μg/mL, 1.0 μg/mL, and 5.0 μg/mL). After being cultured for 24 hours, the culture media were withdrawn and the cells were washed with cold phosphate-buffered saline for harvest. The cell pellets were disrupted in cell radioimmunoprecipitation assay buffer (0.5% NP-40, 50 mM Tris-HCl, 120 mM NaCl, 1 mM EDTA, 0.1 mM Na_3VO_4, 1 mM NaF, 1 mM PMSF, and 1 μg/mL leupeptin, pH 7.5), and then the lysates were centrifuged at 12,000 rpm for 15 minutes at 4°C. The protein concentrations were determined using the BCA method, after an equal amount of protein (30 μg) was electrophoresed on 7.5% density of sodium dodecyl sulfate–acrylamide gels. Following electrophoresis, the proteins were transferred from the gel to a nitrocellulose membrane using an electron transfer system. Nonspecific binding was blocked with 5% skim milk in Tris-buffered saline with Tween 20 (TBST) buffer (5 mM Tris-HCl, 136 mM NaCl, and 0.1% Tween-20, pH 7.6) for 1 hour. The blots were incubated with antibodies against HIF-1α (1:2,000), PHD-2 (1:1,500), or β-actin (1:800) overnight at 4°C and were washed three times with 1× TBST. Then, the blots were incubated for 1 hour at room temperature with a 1:4,000 dilution of horseradish peroxidase-labeled antirabbit or antimouse IgG and washed three times with 1× TBST. The membranes were developed by incubation within the ECL Western blot detection reagents. The specific protein bands (the upper band of HIF-1α and the lower band of PHD-2) were visualized and analyzed with a ChemiDoc image analyzer (Bio-Rad Laboratories Inc., Hercules, CA, USA).

Rat model of oxygen-induced retinopathy

All animal experiments were performed strictly in accordance with the university's guidelines and were approved by the Committee on Use and Care of Animals of Sichuan University (Chengdu, Sichuan, People's Republic of China). Ten pregnant (16–20 weeks old and body weight 300–350 g, for oxygen-induced retinopathy [OIR] model study) Sprague Dawley rats (SPF Grade, Certificate No SCXK2013-24) were purchased from the Experimental Animal Centre, Sichuan Provincial Academy of Medical Sciences in the People's Republic of China (Chengdu, Sichuan, People's Republic of China). OIR was induced in Sprague Dawley rat pups according to a protocol as previously described.[34] In brief, normalized litters of 50 Sprague-Dawley rat pups with their nursing mothers on postnatal day (PD) 7 were placed in an 80% oxygen atmosphere for 5 days. After being returned to normoxia condition for 5 days (on PD 12), the rat pups were intraperitoneally administered with Conbercept injection at 1.0 mg/kg or FMN at 5.0 mg/kg and 10.0 mg/kg, and the same volume of normal saline as control. Five days later

(on PD 17), the rat pups were sacrificed (the pups in the control group were bred under normoxia conditions until PD 17), and the eyes were enucleated and fixed in fresh 4% paraformaldehyde for 2 hours. Eyecups were dissected, and the retinal flat mounts were created and stained with ADPase staining as described previously.[35] The retinal avascular areas were assessed through visualization of the retinal vasculature using infusion of ADPase staining, examined under fluorescent microscopy. In each whole mount, the total areas of preretinal neovascular areas were measured using Image-Pro Plus System and expressed as the percentage of the respective average in relation to total retinal areas. The retinas were also histologically examined. Serial sections of paraffin-embedded small pieces of retina (6 mm) were stained with hematoxylin and eosin. Images were taken under microscopy, and endothelial nuclei extended beyond the inner limiting membrane into the vitreous were manually counted in a blind manner.

Statistical analysis

All the data were reported as mean ± standard deviation. Statistical significance of the data was analyzed by one-way univariate analysis of variance for comparing data from more than two groups. A difference at $P<0.05$ was considered to be statistically significant (marked as *). The higher significance level was set at $P<0.01$ (marked as **). The data were analyzed among the $CoCl_2$-treated groups as one factor and FMN-treated groups as another factor.

Results

FMN inhibits the secretion of VEGF in the ARPE-19 cells under hypoxia condition

FMN is an important compound in *A. membranaceus* for the protection of DR, and the structure is shown in Figure 1. In order to study the effect of FMN on VEGF secretion under hypoxia, ELISA was applied to examine the concentrations of VEGF in the cultured medium of the ARPE-19 cells treated with 150 μM $CoCl_2$ alone or in combination with FMN at 0.2 μg/mL, 1.0 μg/mL, or 5.0 μg/mL. As shown in Figure 2, the level of VEGF in the culture supernatant was significantly increased after the cells were treated with 150 μM $CoCl_2$ compared to the non-$CoCl_2$ cells ($P<0.01$). However, YC-1 at 1.0 μg/mL and FMN at 0.2 μg/mL, 1.0 μg/mL, and 5.0 μg/mL markedly decreased the secretion of VEGF compared to the cells treated with $CoCl_2$ under hypoxia condition ($P<0.01$). These results indicate that FMN inhibits the secretion of VEGF in the culture supernatant of the ARPE-19 cells.

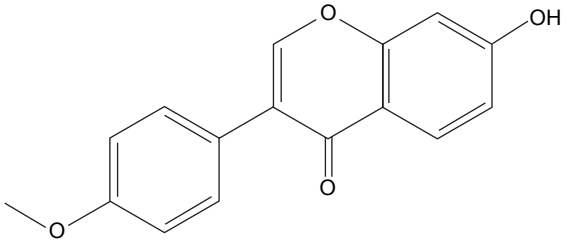

Figure 1 Structure of 7-hydroxy-4′-methoxyisoflavone (FMN).

Effects of FMN on the mRNA expressions of VEGFA, HIF-1α, and PHD-2 in the ARPE-19 cells

The expression of VEGFA can be induced by posttranscriptional mechanisms directed at the VEGFA mRNA or its relative regulator in the pathophysiological states.[36] We hypothesized that FMN may be involved in the mRNA expressions of VEGFA, HIF-1α, and PHD-2. For this purpose, we examined the mRNA expressions of VEGFA, HIF-1α, and PHD-2 in the ARPE-19 cells by qRT-PCR analysis. As shown in Figure 3A, the expression of VEGFA mRNA increased significantly in the ARPE-19 cells treated with 150 μM $CoCl_2$ for 24 hours ($P<0.01$). FMN at 0.2–5.0 μg/mL significantly decreased the high expression of VEGFA mRNA induced by $CoCl_2$ ($P<0.01$) in a dose-dependent manner (Figure 3A), indicating that FMN blocked the elevated expression of VEGFA mRNA induced by hypoxia. The data in Figure 3B show that the combination of 150 μM $CoCl_2$ with YC-1 at 1.0 μg/mL or FMN at 0.2–5.0 μg/mL did not affect the mRNA

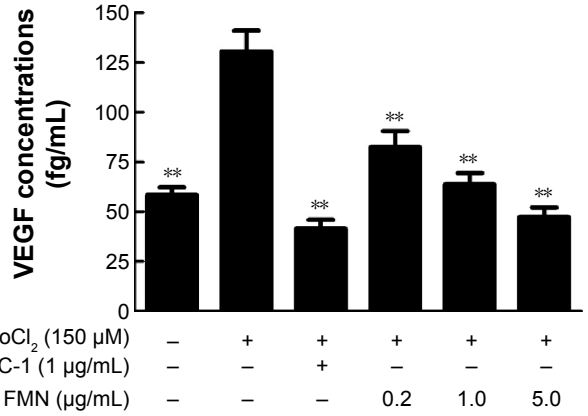

Figure 2 The effects of FMN on VEGF secretion in the ARPE-19 cells at 48 hours under hypoxic condition.

Notes: The results are representative of at least three independent experiments run in triplicate and expressed as mean ± SD. **$P<0.01$ vs $CoCl_2$-treated group. The control cells were treated with a culture medium containing 0.1% DMSO.

Abbreviations: FMN, formononetin; ARPE-19, acute retinal pigment epithelial-19; SD, standard deviation; DMSO, dimethyl sulfoxide.

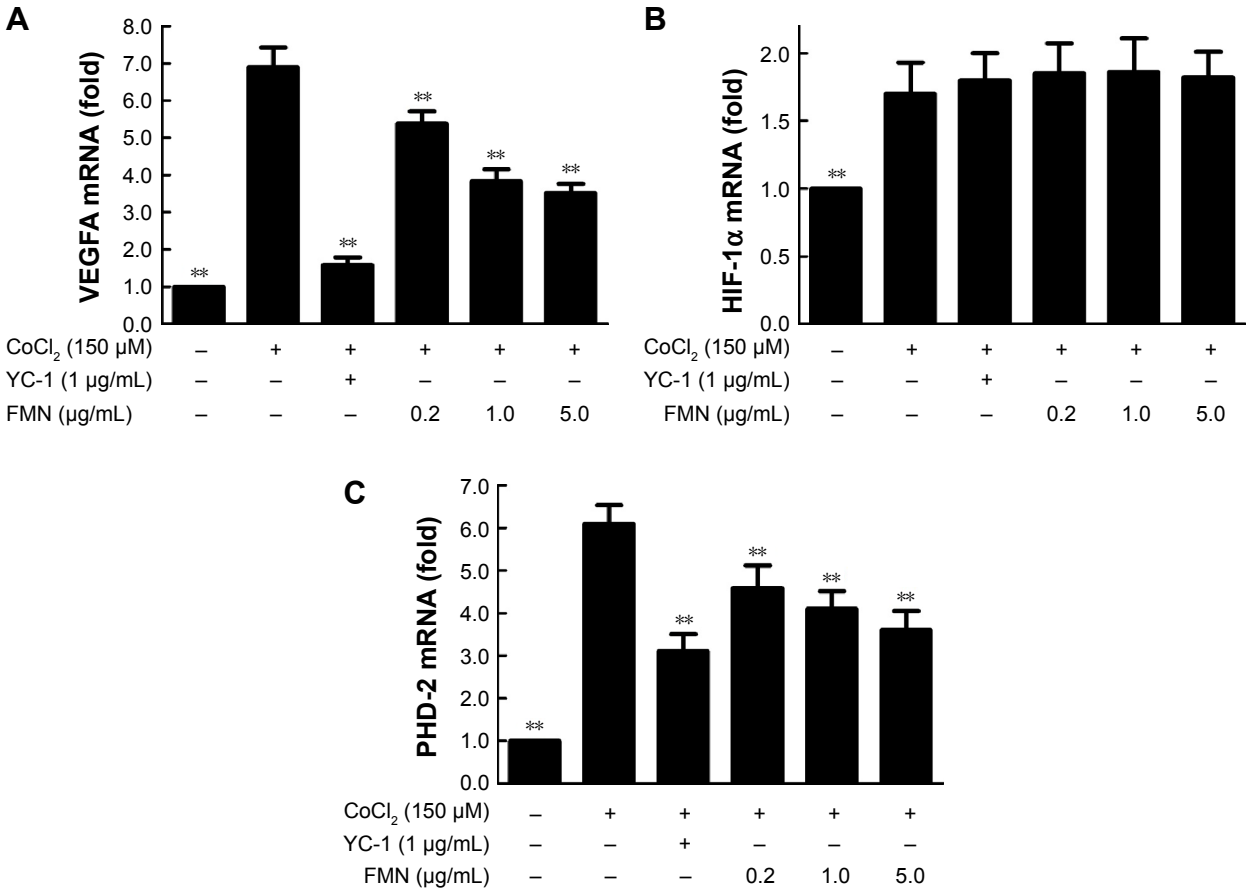

Figure 3 The effects of FMN on the mRNA expressions of VEGFA (**A**), HIF-1α (**B**), and PHD-2 (**C**) in the ARPE-19 cells at 24 hours under normoxia or hypoxic condition.
Notes: The results are representative of at least three independent experiments run in triplicate and expressed as mean ± SD. $^{**}P<0.01$ vs $CoCl_2$-treated cells. The control cells were treated with a culture medium containing 0.1% DMSO.
Abbreviations: FMN, formononetin; ARPE-19, acute retinal pigment epithelial-19; SD, standard deviation; DMSO, dimethyl sulfoxide.

expression of HIF-1α compared to $CoCl_2$ alone. However, the data in Figure 3C show that the mRNA expression of PHD-2 was increased ($P<0.01$) under $CoCl_2$-induced hypoxia-mimicking conditions and was significantly downregulated by YC-1 (1.0 μg/mL) or FMN (0.2–5.0 μg/mL) compared to $CoCl_2$ alone ($P<0.01$). These results show that VEGF expression under hypoxia is associated with the mRNA expressions of VEGFA and PHD-2.

Effects of FMN on the intracellular levels of HIF-1α and PHD-2 protein in the ARPE-19 cells

VEGFA is potently induced by hypoxia and regulated by HIF-1α and its degradation regulator PHD-2.[37] Here, we used the anti-HIF-1α and anti-PHD-2 antibodies to examine the protein expressions of HIF-1α and PHD-2 in the cultured ARPE-19 cells under hypoxia condition. Western blot analysis showed that the protein expressions of HIF-1α and PHD-2 were significantly upregulated in the ARPE-19 cells treated with 150 μM $CoCl_2$ for 24 hours compared to the cells treated with the medium ($P<0.01$) and significantly downregulated by YC-1 (1.0 μg/mL) or FMN (0.2–5.0 μg/mL) compared to $CoCl_2$ alone ($P<0.01$; Figure 4A and B). These results indicate that the inhibition of FMN on VEGF secretion of the ARPE-19 cells under hypoxia condition is associated with the protein expressions of HIF-1α and PHD-2, suggesting a possible mechanism involved in hypoxia-induced retinal NV and related signaling pathways.

FMN inhibits hypoxia-induced retinal NV in vivo

After we demonstrated the inhibitory effect of FMN on VEGF secretion of the ARPE-19 cells in vitro, next, we investigated the preventive effect of FMN on the hypoxia-induced retinal NV with the superficial vascular plexuses, using ADPase staining in a rat pup model. Rat pups were exposed to 80% oxygen from PD 7 to PD 12 to produce retinal vaso-obliteration and then returned to room air.

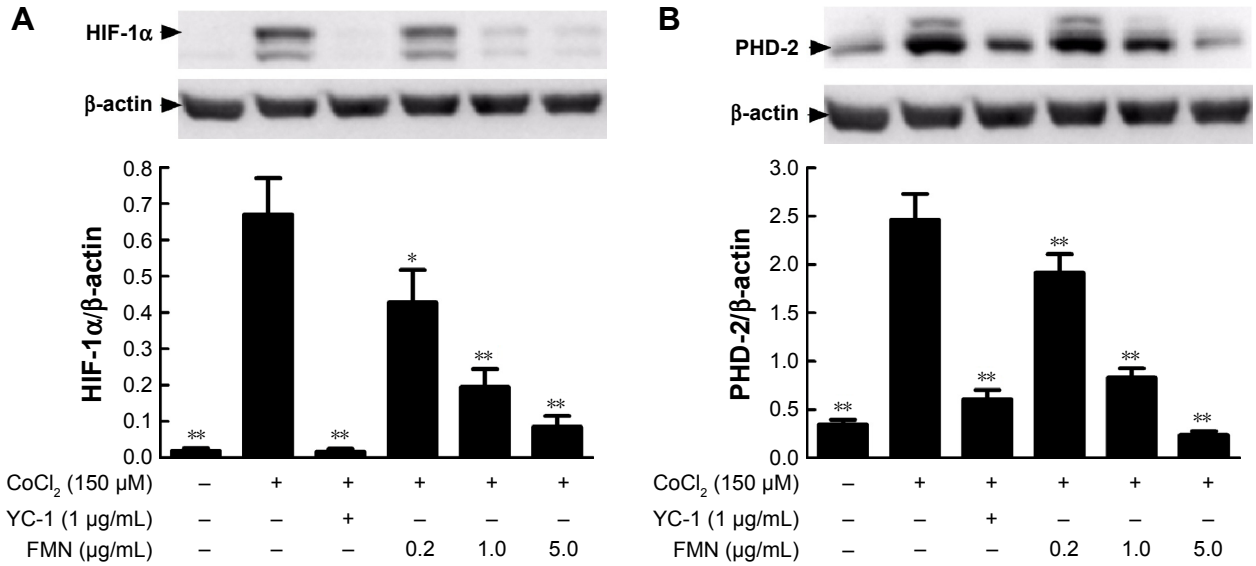

Figure 4 The effects of FMN on the protein expressions of HIF-1α (**A**) and PHD-2 (**B**) in the ARPE-19 cells at 24 hours under normoxia or hypoxic condition.
Notes: The results are representative of at least three independent experiments run in triplicate and expressed as mean ± SD. *$P<0.05$, **$P<0.01$ vs $CoCl_2$-treated cells. The control cells were treated with a culture medium containing 0.1% DMSO.
Abbreviations: FMN, formononetin; ARPE-19, acute retinal pigment epithelial-19; SD, standard deviation; DMSO, dimethyl sulfoxide.

This condition made the retina relatively hypoxic, resulting in the formation of retinal NV. On the PD 17, the preretinal neovascular area ratio was significantly increased in the OIR rats treated with vehicle (saline) compared to that of the normal rats treated with vehicle ($P<0.01$). However, Conbercept (1 mg/kg) or FMN (5 mg/kg and 10 mg/kg) by intraperitoneal injection markedly reversed the hypoxia-induced neovascular area ration and inhibited retinal NV (Figure 5A and B). Furthermore, Conbercept and FMN alleviated NV, vessel tortuosity, and dilated vessels in the OIR rats significantly (Figure 6).

In order to further confirm the inhibitory effect of FMN on retinal NV, we counted the vascular cell nuclei extended beyond the internal limiting membrane in the retinal tissue sections of rats, with hematoxylin and eosin stain. Nuclei anterior to the internal limiting membrane were not found in the retinal tissue sections of the control rats (Figure 7A), but a lot of neovascular nuclei and vessels were found in the retinal tissue sections of the OIR rats (Figure 7B). Interestingly, the neovascular nuclei and vessels in the retinal tissue sections were remarkably reduced by Conbercept (1 mg/kg) or FMN (5 mg/kg and 10 mg/kg) treatment (Figure 7C and D).

Discussion

The present study aimed to investigate whether FMN can prevent hypoxia-induced retinal NV, and the role of

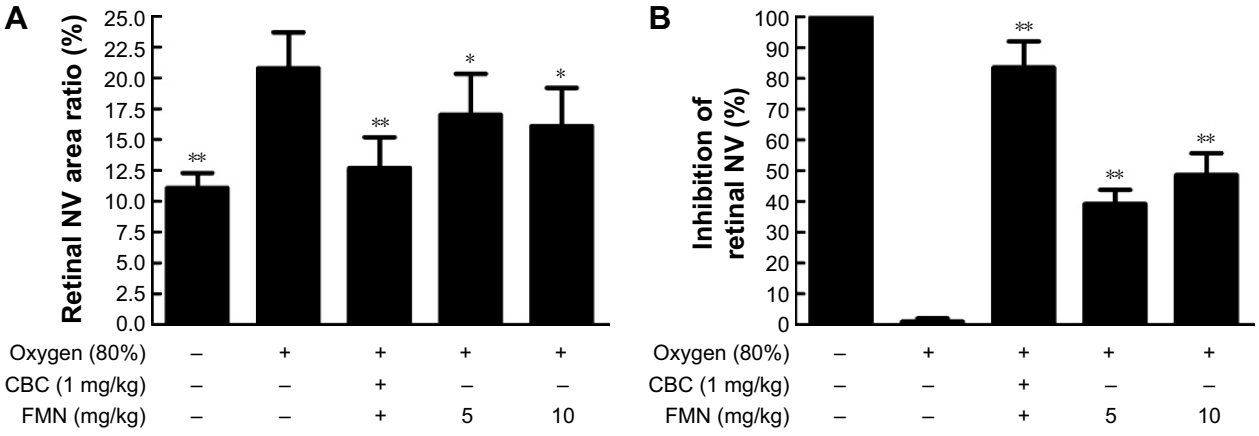

Figure 5 The effects of FMN on quantification of preretinal neovascular area ratio in the OIR rats.
Notes: (**A**) Retinal NV area ration. (**B**) Inhibition of retinal neovascular area. The results were expressed as mean ± SD (n=10). *$P<0.05$, **$P<0.01$, compared to the OIR rats.
Abbreviations: FMN, formononetin; OIR, oxygen-induced retinopathy; NV, neovascularization; SD, standard deviation; CBC, conbercept ophthalmic injection.

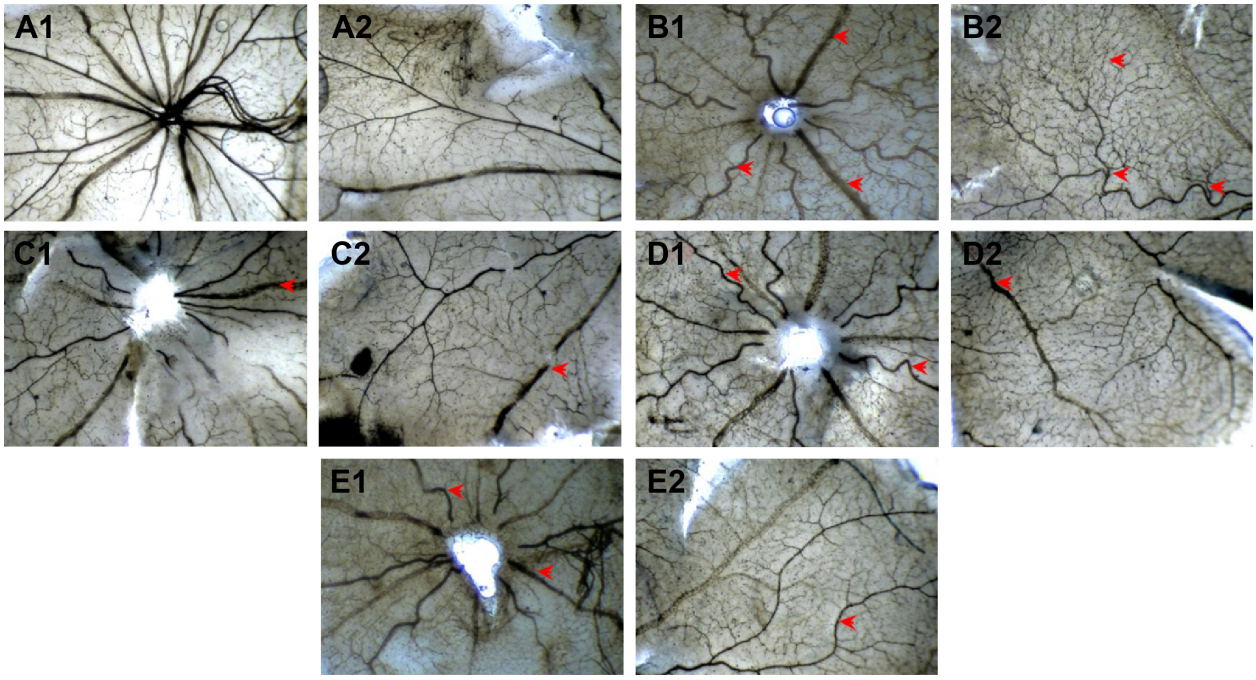

Figure 6 The effects of Conbercept and FMN on retinal NV of the OIR rats in the ADPase-stained retinal sections (40×).
Notes: Central retinal region (**A1**–**E1**) and peripheral retinal region (**A2**–**E2**) of rat pups fostered under normoxia conditions (control), and OIR rats under 80% oxygen. The rats were treated with normal saline (control), 1.0 mg/kg Conbercept, and 5.0 mg/kg or 10.0 mg/kg FMN by ip injection. Ten rats were used for each group. The red arrowhead shows the vessel tortuosity, and dilated vessels.
Abbreviations: FMN, formononetin; NV, neovascularization; OIR, oxygen-induced retinopathy; ADP, adenosine diphosphate; ip, intraperitoneal.

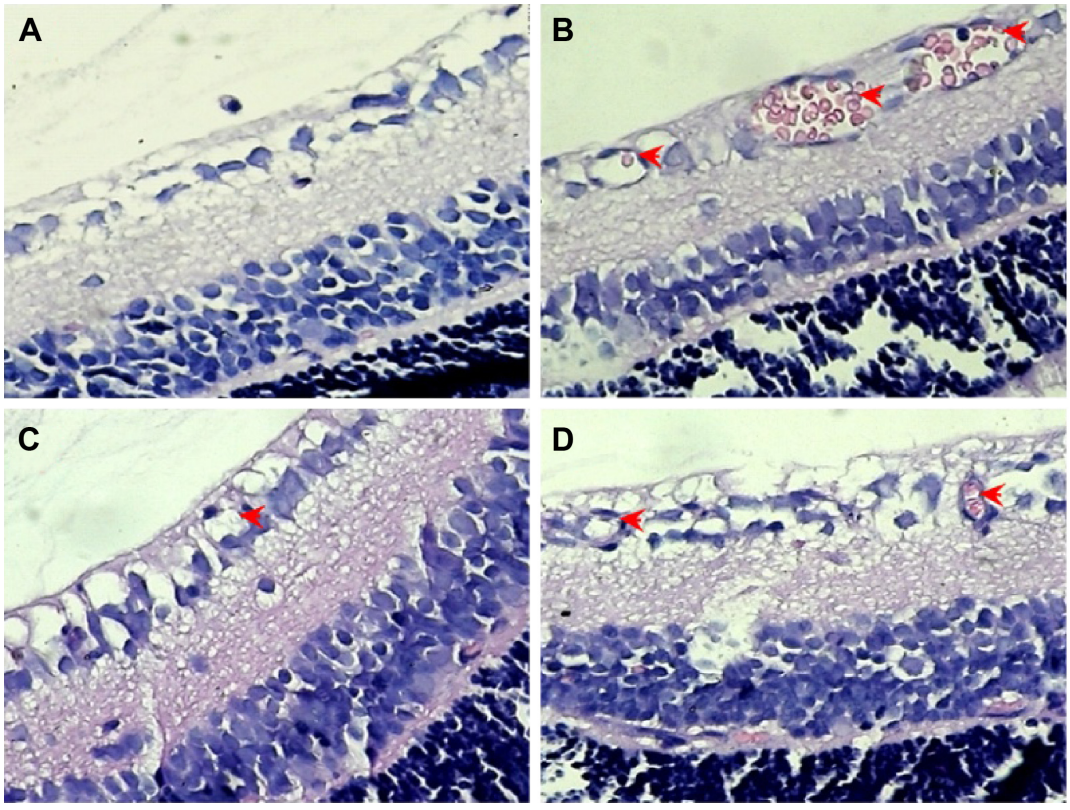

Figure 7 The effects of FMN on retinal NV in H&E-stained retinal tissue sections (×400).
Notes: (**A**) Control group, rat pups fostered under normoxia conditions, (**B**) treated with normal saline (**C**) treated with 1.0 mg/kg Conbercept, (**D**) treated with 10.0 mg/kg FMN OIR rats under 80% oxygen. The rats were treated with normal saline (control), 1.0 mg/kg Conbercept, or 10.0 mg/kg FMN by ip injection. Ten rats were used for each group. Red arrows indicate neovascular nuclei or vessel.
Abbreviations: FMN, formononetin; NV, neovascularization; H&E, hematoxylin and eosin; OIR, oxygen-induced retinopathy; ip, intraperitoneal.

HIF-1α/VEGF signaling pathway. We applied the VEGF secretion model of ARPE-19 cells induced by $CoCl_2$ in vitro, and NV rat model of oxygen-induced retinopathy in vivo. Our results reveal that FMN can indeed inhibit VEGF secretion of the ARPE-19 cells under hypoxia condition, downregulate mRNA expressions of VEGFA and PHD-2, and decrease the protein expressions of VEGF, HIF-1α, and PHD-2 in vitro. Furthermore, the results also show that FMN can prevent hypoxia-induced retinal NV in vivo. The results show that FMN can alleviate hypoxia-induced retinal angiogenesis through suppression of the HIF-1α/VEGF signaling pathway (Figure 8). Therefore, our findings suggest that FMN is effective against DR and may potentially be developed as a natural drug for the treatment of DR. However, the pharmacological effects on other animal models and the associated mechanism(s) against DR need to be further investigated.

VEGF plays a key role in the retinal NV in the pathological process of DR, including angiogenesis, vasculogenesis, endothelial cell growth, and so on. Meanwhile, retinal pigment epithelium cells located between the photoreceptors and choriocapillaris (capillaries forming the inner vascular layer of the choroid) play an important role in maintaining retinal homeostasis and VEGF production within the area of blood–ocular barrier.[30,38,39] In the present study, we employed $CoCl_2$, a widely used chemical compound, to mimic hypoxia condition in the cultured ARPE-19 cells to study the regulation of VEGF expression. Our data revealed that exposure of 150 mM $CoCl_2$ to the cells significantly increased mRNA expression at 24 hours and markedly increased the VEGF secretion at 48 hours. The different response times with $CoCl_2$ exposure may result because the mRNA transcription and translation and secretion of VEGF occurred at different times. Furthermore, our data demonstrate that FMN can simultaneously inhibit the mRNA transcription and protein expression of VEGF. This finding is consistent with the previous study of antiangiogenesis on the tumor with high

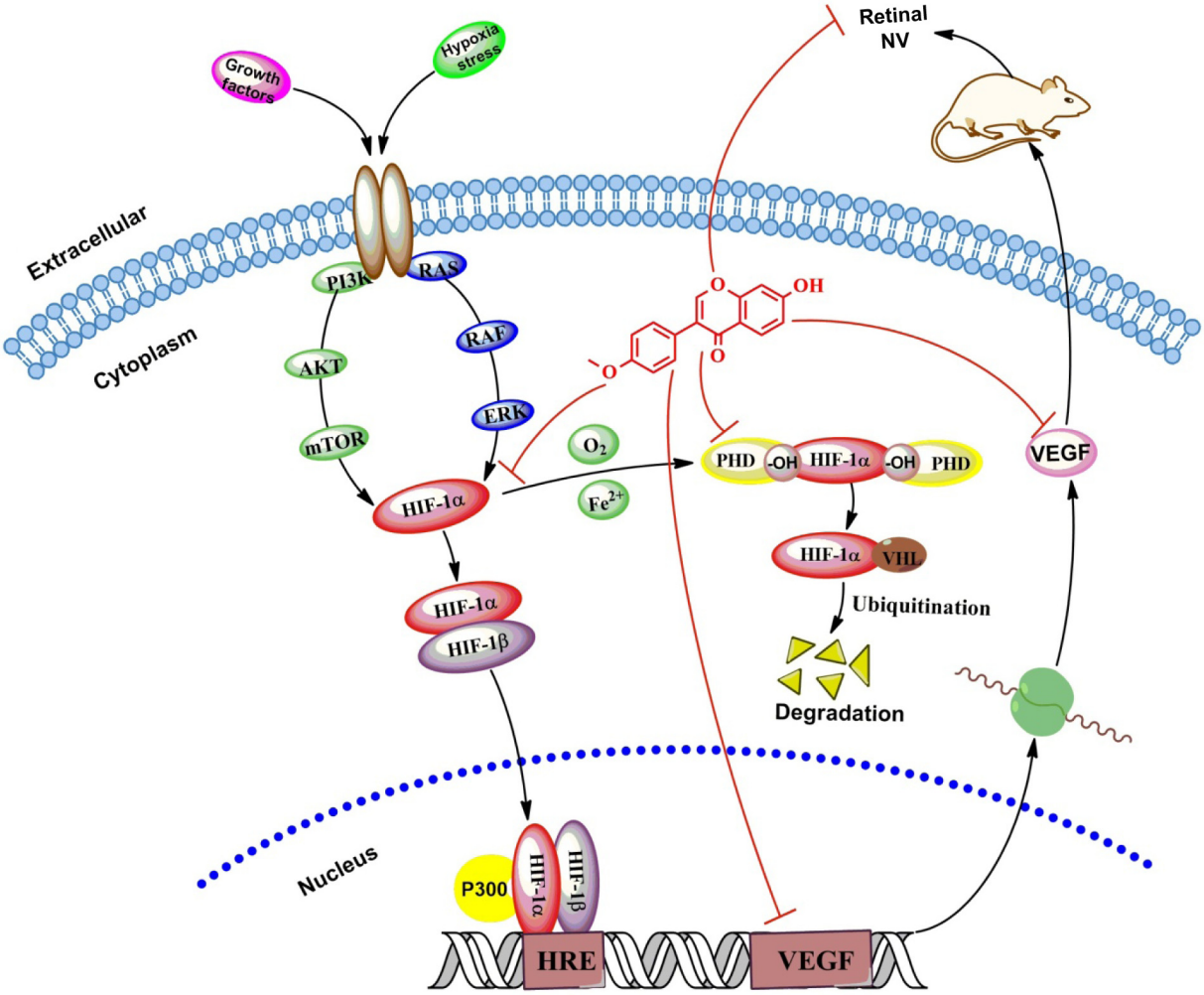

Figure 8 FMN alleviates hypoxia-induced retinal angiogenesis through suppression of the HIF-1α/VEGF signaling pathway.
Abbreviations: FMN, formononetin; NV, neovascularization.

expression of VEGF.[21] However, FMN also can contrarily promote angiogenesis through estrogen receptor or MAPK pathway in human pancreatic tumor cells with low expression of VEGF.[40] The possible reasons for the difference may be due to the diverse pathophysiologic foundation with different VEGF expression levels, or FMN as a natural selective estrogen receptor modulator and/or ligand for the GR and estrogen receptor (ER), to exhibit the angiogenic or antiangiogenic effect in the different pathophysiologic states as a bidirectionally regulative effect of *A. membranaceus*.[41]

HIF is a heterodimeric transcriptional factor that is activated and stabilized under hypoxic condition. HIF promotes the expressions of gene products, including angiogenesis factors (eg, VEGF and TGF-β_3), erythropoiesis factors (eg, EPO), cell survival, and proliferation factors (eg, IGF-2, ID2, and NOS).[37,42–46] Meanwhile, HIF-1 is composed of two subunits of HIF-1α and HIF-1β. HIF-1α is an oxygen-sensitive subunit, and its expression is induced under hypoxic conditions. In contrast, HIF-1β is constitutively expressed. HIF-1β is also known as aryl hydrocarbon nuclear translocator, because it needs to bind with HIF-1α and AhR, facilitating its translocation to the nucleus.[37] However, HIF-1α can be hydroxylated by HIF PHDs (especially PHD-2) in normoxia; the hydroxylated HIF-1α is multiubiquitinated and degraded in the proteasome. Conversely, the mRNA expression of PHD-2 is upregulated by hypoxia through an HIF-1α-dependent signaling pathway.[47] In addition, the PHD activity is inhibited under low oxygen tension.[48] This counter action could explain why the expression of PHD-2 is upregulated by $CoCl_2$ and downregulated by FMN through inhibition of HIF-1α protein expression, as previously reported.[49] In the present study, we found the mRNA expressions of VEGF and PHD-2 and the protein expressions of VEGF, HIF-1α, and PHD-2 can be induced by $CoCl_2$ under hypoxia conditions. Meanwhile, FMN can inhibit the increase induced by $CoCl_2$ in a dose-dependent manner. FMN inhibited the secretion of VEGF via the HIF-1α/VEGF signaling pathway. In order to demonstrate the inhibitory effect of FMN on retinal NV in vivo, the rat model of oxygen-induced retinopathy was used to investigate the pharmacological effect of FMN on ischemic retinopathy induced by hyperoxia and followed by returning to normoxia as the literature reported.[34] Increased retinal NV was found in the OIR rats, and FMN significantly alleviated the NV, vessel tortuosity, and dilated vessels in the OIR rats, suggesting that FMN may be a potent inhibitor of retinal NV via the HIF-1α/VEGF signaling pathway.

Actually, HIF-1α undergoes quick degradation under normoxic condition and normally has a very short half-life (~5 minutes).[50] In contrast, in hypoxic conditions, several pathways have been shown to control HIF-1α stability and transcriptional activity via posttransnational modifications involving hydroxylation, acetylation, ubiquitination, and phosphorylation reactions, including hypoxic regulation pathway (pVHL dependent or pVHL independent),[51] growth factor signaling pathway,[52] Mdm2 pathway,[53] Hsp90 pathway, and so on.[54] Therefore, our further investigation into the molecular mechanisms associated with the effects of FMN on anti-retinal NV should include the study of upstream regulation, degradation of HIF-1α, and HRE transcription.

Conclusion

In the present study, we reveal that FMN plays an important role in the inhibition of VEGF secretion, through downregulating the mRNA expressions of VEGFA and PHD-2 and decreasing the protein expressions of VEGF, HIF-1α, and PHD-2 in the cultured ARPE-19 cells. Furthermore, we also demonstrate the inhibitory effect of FMN on retinal NV in a rat model of oxygen-induced retinopathy in vivo. These results may provide important insights into potential discovery and development of FMN as a novel drug for the treatment of DR clinically. However, more studies are needed to further investigate the pharmacological effects in other animal models and the possible associated mechanism(s) against DR.

Acknowledgments

The authors thank Professor Shousong Cao (Southwest Medical University) for proof reading and editing of the manuscript. This work was supported by Technology Support Program of Science and Technology, Department of Sichuan Province, People's Republic of China (2012SZ0038).

Author contributions

Jianming Wu, Xiao Ke, Xiaoping Gao, and Xiaofeng Hao conceived and designed the experiments; Jianming Wu, Wei Fu, Hongcheng Zhang, Wei Wang, Na Ma, and Manxi Zhao performed the experiments; Jianming Wu, Manxi Zhao, and Xiaoping Gao analyzed the data; Xiao Ke, Xiaofeng Hao, and Zhirong Zhang contributed new reagents and analysis tools; and Jianming Wu and Zhirong Zhang wrote the article. All authors contributed toward data analysis, drafting and critically revising the paper and agree to be accountable for all aspects of the work.

Disclosure

The authors report no conflicts of interest in this work.

References

1. Fu J, Wang Z, Huang L, et al. Review of the botanical characteristics, phytochemistry, and pharmacology of *Astragalus membranaceus* (Huangqi). *Phytother Res*. 2014;28(9):1275–1283.
2. Zhang J, Xie X, Li C, Fu P. Systematic review of the renal protective effect of *Astragalus membranaceus* (root) on diabetic nephropathy in animal models. *J Ethnopharmacol*. 2009;126(2):189–196.
3. Cho WC, Leung KN. In vitro and *in vivo* immunomodulating and immunorestorative effects of *Astragalus membranaceus*. *J Ethnopharmacol*. 2007;113(1):132–141.
4. Yang B, Xiao B, Sun T. Antitumor and immunomodulatory activity of *Astragalus membranaceus* polysaccharides in H22 tumor-bearing mice. *Int J Biol Macromol*. 2013;62:287–290.
5. Chen SM, Tsai YS, Lee SW, et al. *Astragalus membranaceus* modulates Th1/2 immune balance and activates PPARgamma in a murine asthma model. *Biochem Cell Biol*. 2014;92(5):397–405.
6. Agyemang K, Han L, Liu E, Zhang Y, Wang T, Gao X. Recent advances in *Astragalus membranaceus* anti-diabetic research: pharmacological effects of its phytochemical constituents. *Evid Based Complement Alternat Med*. 2013;2013:654643.
7. Mao XQ, Yu F, Wang N, et al. Hypoglycemic effect of polysaccharide enriched extract of *Astragalus membranaceus* in diet induced insulin resistant C57BL/6J mice and its potential mechanism. *Phytomedicine*. 2009;16(5):416–425.
8. Zou F, Mao XQ, Wang N, Liu J, Ou-Yang JP. Astragalus polysaccharides alleviates glucose toxicity and restores glucose homeostasis in diabetic states *via* activation of AMPK. *Acta Pharmacol Sin*. 2009; 30(12):1607–1615.
9. Ko JK, Chik CW. The protective action of radix *Astragalus membranaceus* against hapten-induced colitis through modulation of cytokines. *Cytokine*. 2009;47(2):85–90.
10. Lai PK, Chan JY, Wu SB, et al. Anti-inflammatory activities of an active fraction isolated from the root of *Astragalus membranaceus* in RAW 264.7 macrophages. *Phytother Res*. 2014;28(3):395–404.
11. Jiao J, Gai QY, Wang W, et al. Ultraviolet radiation-elicited enhancement of isoflavonoid accumulation, biosynthetic gene expression, and antioxidant activity in *Astragalus membranaceus* hairy root cultures. *J Agric Food Chem*. 2015;63(37):8216–8224.
12. Shahzad M, Shabbir A, Wojcikowski K, Wohlmuth H, Gobe GC. The antioxidant effects of Radix Astragali (*Astragalus membranaceus* and related species) in protecting tissues from injury and disease. *Curr Drug Targets*. Epub 2015 Sep 6.
13. Jin M, Zhao K, Huang Q, Shang P. Structural features and biological activities of the polysaccharides from *Astragalus membranaceus*. *Int J Biol Macromol*. 2014;64:257–266.
14. Sun Y, Yang J. Experimental study of the effect of *Astragalus membranaceus* against herpes simplex virus type 1. *Di Yi Jun Yi Da Xue Xue Bao*. 2004;24(1):57–58.
15. Sun WY, Wei W, Gui SY, et al. Protective effect of extract from *Paeonia lactiflora* and *Astragalus membranaceus* against liver injury induced by bacillus Calmette-Guerin and lipopolysaccharide in mice. *Basic Clin Pharmacol Toxicol*. 2008;103(2):143–149.
16. Sun WY, Wang L, Liu H, Li X, Wei W. A standardized extract from *Paeonia lactiflora* and *Astragalus membranaceus* attenuates liver fibrosis induced by porcine serum in rats. *Int J Mol Med*. 2012;29(3): 491–498.
17. Luo Z, Zhong L, Han X, Wang H, Zhong J, Xuan Z. *Astragalus membranaceus* prevents daunorubicin-induced apoptosis of cultured neonatal cardiomyocytes: role of free radical effect of Astragalus membranaceus on daunorubicin cardiotoxicity. *Phytother Res*. 2009;23(6):761–767.
18. Sun M, Zhou T, Zhou L, et al. Formononetin protects neurons against hypoxia-induced cytotoxicity through upregulation of ADAM10 and sAβPPα. *J Alzheimers Dis*. 2012;28(4):795–808.
19. Ma Z, Ji W, Fu Q, Ma S. Formononetin inhibited the inflammation of LPS-induced acute lung injury in mice associated with induction of PPAR gamma expression. *Inflammation*. 2013;36(6):1560–1566.
20. Wang H, Zhang D, Ge M, et al. Formononetin inhibits enterovirus 71 replication by regulating COX-2/PGE(2) expression. *Virol J*. 2015;12:35.
21. Wu XY, Xu H, Wu ZF, et al. Formononetin, a novel FGFR2 inhibitor, potently inhibits angiogenesis and tumor growth in preclinical models. *Oncotarget*. 2015;6(42):44563–44578.
22. Zhang S, Tang X, Tian J, et al. Cardioprotective effect of sulphonated formononetin on acute myocardial infarction in rats. *Basic Clin Pharmacol Toxicol*. 2011;108(6):390–395.
23. Li C, Zhou W, Wang Z, et al. Huangqi injection attenuates the pancreatic β-cells damage in streptozotocin-induced diabetic rats. *Int Med J*. 2014;21(2):211–214.
24. Hu JF, Wang W, Wu JM, et al. Inhibitory effects of Keluoxin capsule on hypoxia-induced angiogenesis in retina. *Chin J Exp Tradit Med Form*. 2014;20(10):156–160.
25. Vaziri K, Schwartz SG, Relhan N, Kishor KS, Flynn HW Jr. New therapeutic approaches in diabetic retinopathy. *Rev Diabet Stud*. 2015; 12(1–2):196–210.
26. Jo DH, An H, Chang DJ, et al. Hypoxia-mediated retinal neovascularization and vascular leakage in diabetic retina is suppressed by HIF-1alpha destabilization by SH-1242 and SH-1280, novel hsp90 inhibitors. *J Mol Med (Berl)*. 2014;92(10):1083–1092.
27. Sugimoto M, Cutler A, Shen B, et al. Inhibition of EGF signaling protects the diabetic retina from insulin-induced vascular leakage. *Am J Pathol*. 2013;183(3):987–995.
28. Rosen R, Vagaggini T, Chen Y, et al. Zeaxanthin inhibits hypoxia-induced VEGF secretion by RPE cells through decreased protein levels of hypoxia-inducible factors-1alpha. *Biomed Res Int*. 2015; 2015:687386.
29. Pages G, Pouyssegur J. Transcriptional regulation of the vascular endothelial growth factor gene – a concert of activating factors. *Cardiovasc Res*. 2005;65(3):564–573.
30. Kurihara T, Westenskow PD, Friedlander M. Hypoxia-inducible factor (HIF)/vascular endothelial growth factor (VEGF) signaling in the retina. *Adv Exp Med Biol*. 2014;801:275–281.
31. Kim JH, Kim JH, Yu YS, Shin JY, Lee HY, Kim KW. Deguelin inhibits retinal neovascularization by down-regulation of HIF-1alpha in oxygen-induced retinopathy. *J Cell Mol Med*. 2008;12(6):2407–2415.
32. DeNiro M, Al-Halafi A, Al-Mohanna FH, Alsmadi O, Al-Mohanna FA. Pleiotropic effects of YC-1 selectively inhibit pathological retinal neovascularization and promote physiological revascularization in a mouse model of oxygen-induced retinopathy. *Mol Pharmacol*. 2010;77(3): 348–367.
33. Iwase T, Fu J, Yoshida T, et al. Sustained delivery of a HIF-1 antagonist for ocular neovascularization. *J Control Release*. 2013;172(3): 625–633.
34. Ricci B. Oxygen-induced retinopathy in the rat model. *Doc Ophthalmol*. 1990;74(3):171–177.
35. Winners-Mendizabal OG, Orge FH, Di Fiore JM, Martin RJ, Kc P. Hypoxia-hyperoxia paradigms in the development of oxygen-induced retinopathy in a rat pup model. *J Neonatal Perinatal Med*. 2014;7(2): 113–117.
36. Osera C, Martindale JL, Amadio M, et al. Induction of VEGFA mRNA translation by $CoCl_2$ mediated by HuR. *RNA Biol*. 2015;12(10): 1121–1130.
37. Masoud GN, Li W. HIF-1alpha pathway: role, regulation and intervention for cancer therapy. *Acta Pharm Sin B*. 2015;5(5):378–389.
38. Marneros AG, Fan J, Yokoyama Y, et al. Vascular endothelial growth factor expression in the retinal pigment epithelium is essential for choriocapillaris development and visual function. *Am J Pathol*. 2005;167(5): 1451–1459.
39. Le YZ, Bai Y, Zhu M, Zheng L. Temporal requirement of RPE-derived VEGF in the development of choroidal vasculature. *J Neurochem*. 2010; 112(6):1584–1592.
40. Lyn-Cook BD, Stottman HL, Yan Y, Blann E, Kadlubar FF, Hammons GJ. The effects of phytoestrogens on human pancreatic tumor cells in vitro. *Cancer Lett*. 1999;142(1):111–119.

41. Kaczmarczyk-Sedlak I, Wojnar W, Zych M, Ozimina-Kamińska E, Taranowicz J, Siwek A. Effect of formononetin on mechanical properties and chemical composition of bones in rats with ovariectomy-induced osteoporosis. *Evid Based Complement Alternat Med*. 2013; 2013:457052.
42. Zhang W, Petrovic JM, Callaghan D, et al. Evidence that hypoxia-inducible factor-1 (HIF-1) mediates transcriptional activation of interleukin-1beta (IL-1beta) in astrocyte cultures. *J Neuroimmunol*. 2006; 174(1–2):63–73.
43. Filippi I, Carrarelli P, Luisi S, et al. Different expression of hypoxic and angiogenic factors in human endometriotic lesions. *Reprod Sci*. 2016;23(4):492–497.
44. Jelkmann W. Regulation of erythropoietin production. *J Physiol*. 2011; 589(6):1251–1258.
45. Thomas R, Kim MH. HIF-1 alpha: a key survival factor for serum-deprived prostate cancer cells. *Prostate*. 2008;68(13):1405–1415.
46. Krotova K, Patel JM, Block ER, Zharikov S. Hypoxic upregulation of arginase II in human lung endothelial cells. *Am J Physiol Cell Physiol*. 2010;299(6):C1541–C1548.
47. Berra E, Benizri E, Ginouvès A, Volmat V, Roux D, Pouysségur J. HIF prolyl-hydroxylase 2 is the key oxygen sensor setting low steady-state levels of HIF-1alpha in normoxia. *EMBO J*. 2003;22(16):4082–4090.
48. Brito LG, Schiavon VF, Andrade JM, et al. Expression of hypoxia-inducible factor 1-alpha and vascular endothelial growth factor-C in locally advanced breast cancer patients. *Clinics (Sao Paulo)*. 2011;66(8): 1313–1320.
49. Carroll VA, Ashcroft M. Role of hypoxia-inducible factor (HIF)-1alpha versus HIF-2alpha in the regulation of HIF target genes in response to hypoxia, insulin-like growth factor-I, or loss of von Hippel-Lindau function: implications for targeting the HIF pathway. *Cancer Res*. 2006; 66(12):6264–6270.
50. Salceda S, Caro J. Hypoxia-inducible factor 1alpha (HIF-1alpha) protein is rapidly degraded by the ubiquitin-proteasome system under normoxic conditions. Its stabilization by hypoxia depends on redox-induced changes. *J Biol Chem*. 1997;272(36):22642–22647.
51. Tug S, Delos Reyes B, Fandrey J, Berchner-Pfannschmidt U. Non-hypoxic activation of the negative regulatory feedback loop of prolyl-hydroxylase oxygen sensors. *Biochem Biophys Res Commun*. 2009; 384(4):519–523.
52. Kaidi A, Qualtrough D, Williams AC, Paraskeva C. Direct transcriptional up-regulation of cyclooxygenase-2 by hypoxia-inducible factor (HIF)-1 promotes colorectal tumor cell survival and enhances HIF-1 transcriptional activity during hypoxia. *Cancer Res*. 2006;66(13):6683–6691.
53. Zhou CH, Zhang XP, Liu F, Wang W. Modeling the interplay between the HIF-1 and p53 pathways in hypoxia. *Sci Rep*. 2015;5:13834.
54. Eschricht S, Jarr KU, Kuhn C, et al. Heat-shock-protein 90 protects from downregulation of HIF-1alpha in calcineurin-induced myocardial hypertrophy. *J Mol Cell Cardiol*. 2015;85:117–126.